Advances in the description of spontaneous fission of transfermium nuclei

T. M. Shneidman
A. Rahmatinejad, A.V. Andreev, G.G. Adamian, N. V. Antonenko

June 19, 2025

Bogoliubov Laboratory of Theoretical Physics,
Joint Institute for Nuclear Research

Table of contents

* Recent experimental developments
* Improved scission point model with random walk
* Distribution of SF observables:
  - Neutron multiplicities
  - SF of $^{244-260}$Fm
* Angular motion at scission
* Correlations between spins of FF and other fission observables for ^{252}Cf
  - Independence of spins of FF
  - Spin versus fragment mass
  - Spin versus TKE
* Conclusion

Measurements of neutron multiplicities at SFiNx

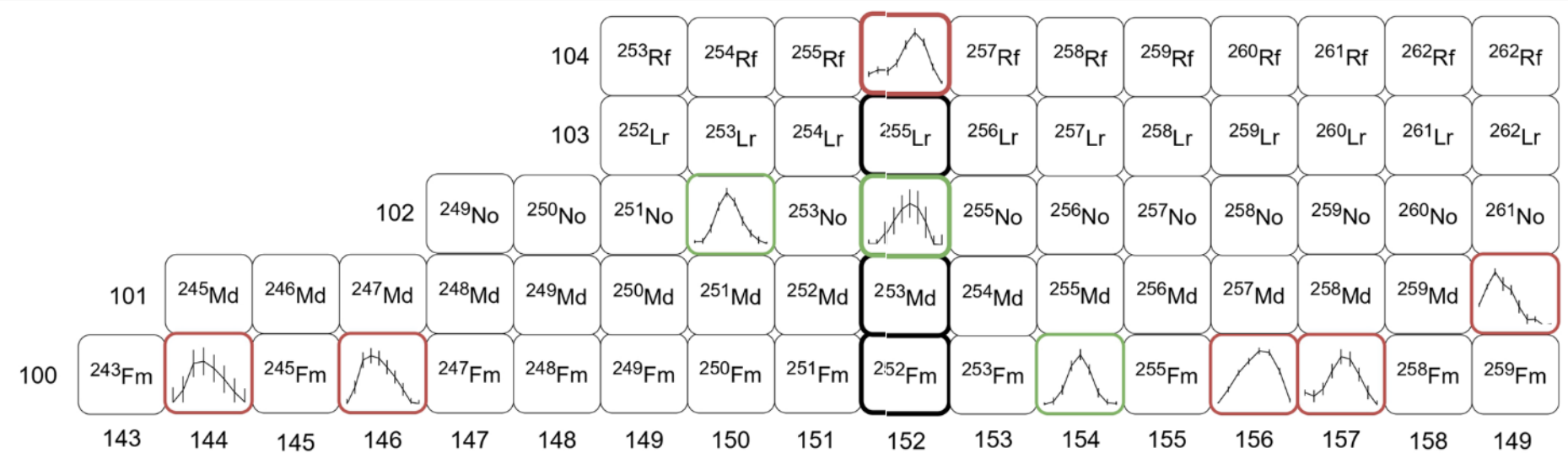

R.S. Mukhin et al., CPC **48**, 064002 (2024).

A.V. Isaev, et al., PLB **843**, 138008 (2023).

A. V. Isaev, EPJA, **58** 108 (2022).

R.S. Mukhin et al., Phys. Part. Nucl. Lett. **18**, 439 (2021).

Systematics of mass distributions in SF of Cm, Cf, Fm, No, and Rf

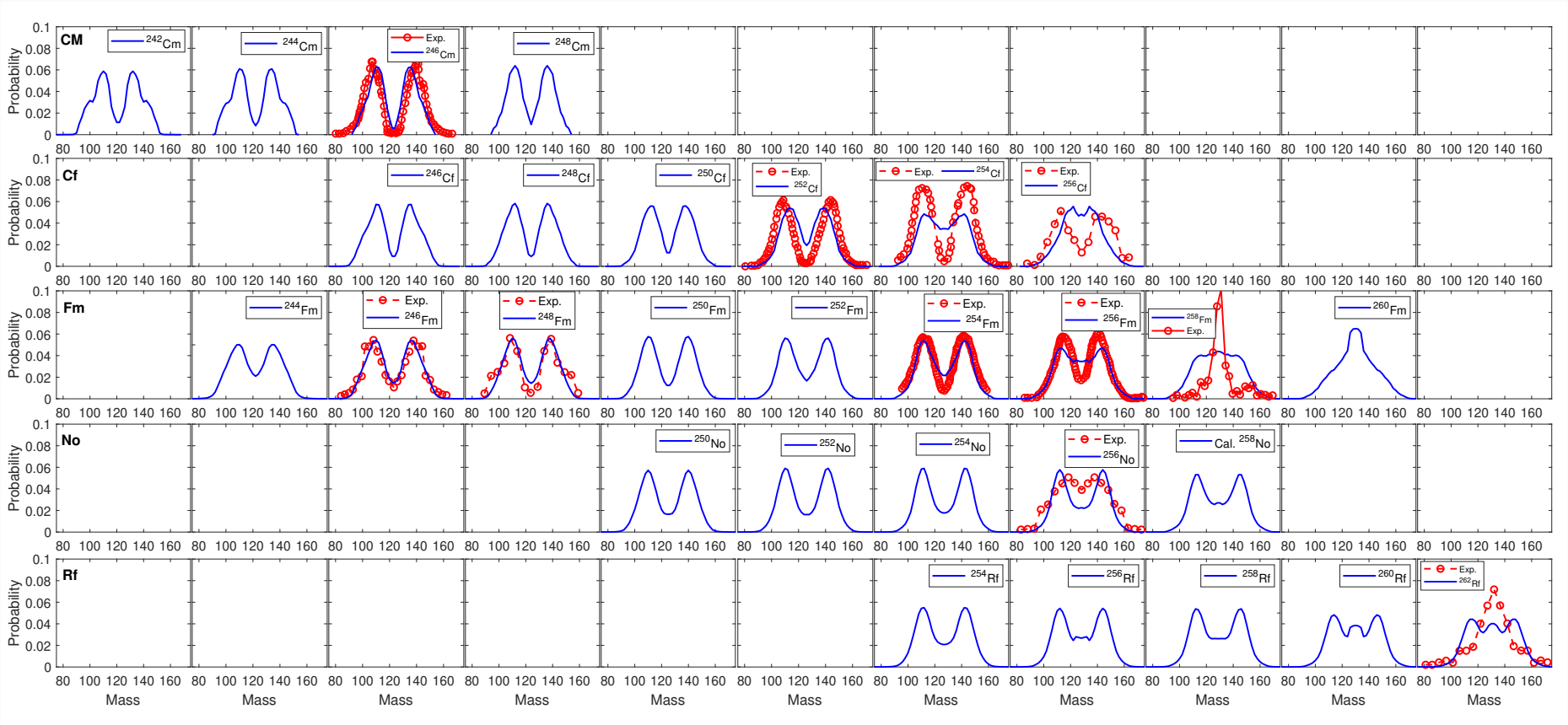

Neutrons versus mass and TKE for SF ^{252}Cf

The distribution of available energy at scission between the excitation and deformation energy of the fragments is particularly decisive in describing correlations between observables.

A. Göök et al., Phys. Rev. C **90**, 064611 (2014).

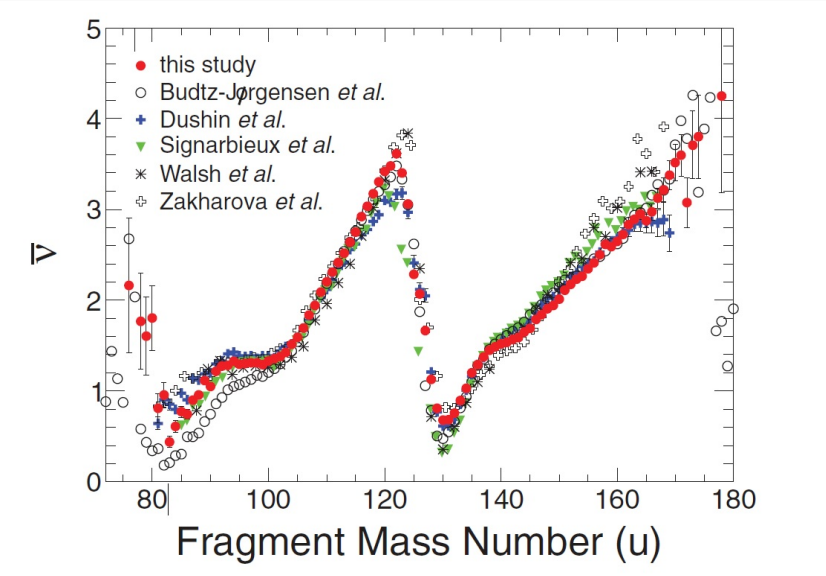

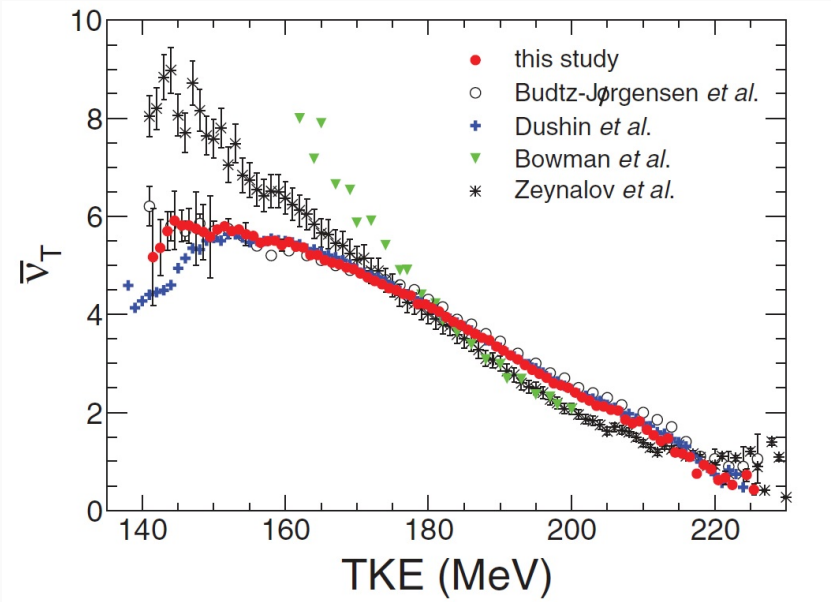

Spins of the fragments

J. N. Wilson et. al, Nature **590**, 566–570 (2021).

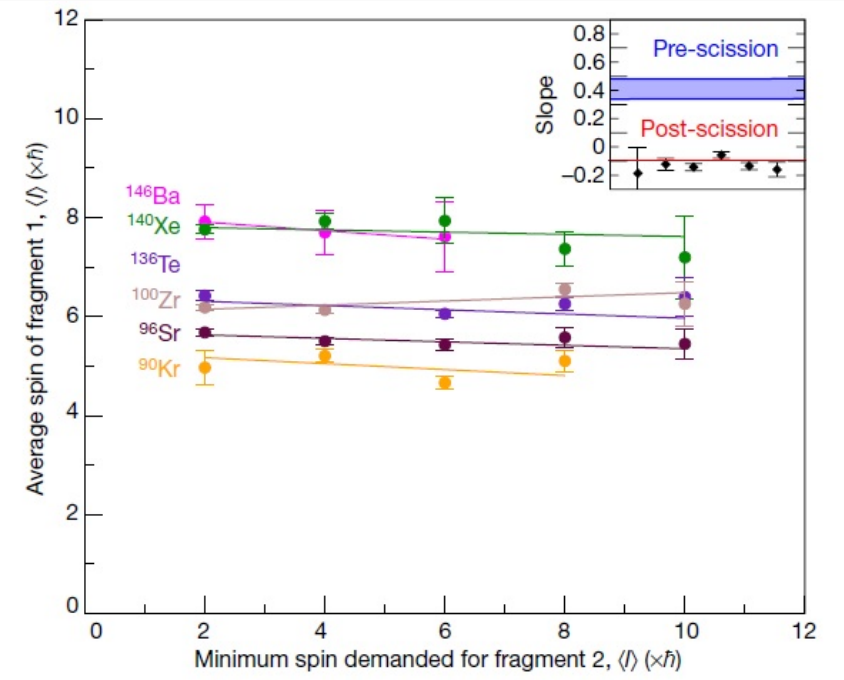

Absence correlation between fragment spins

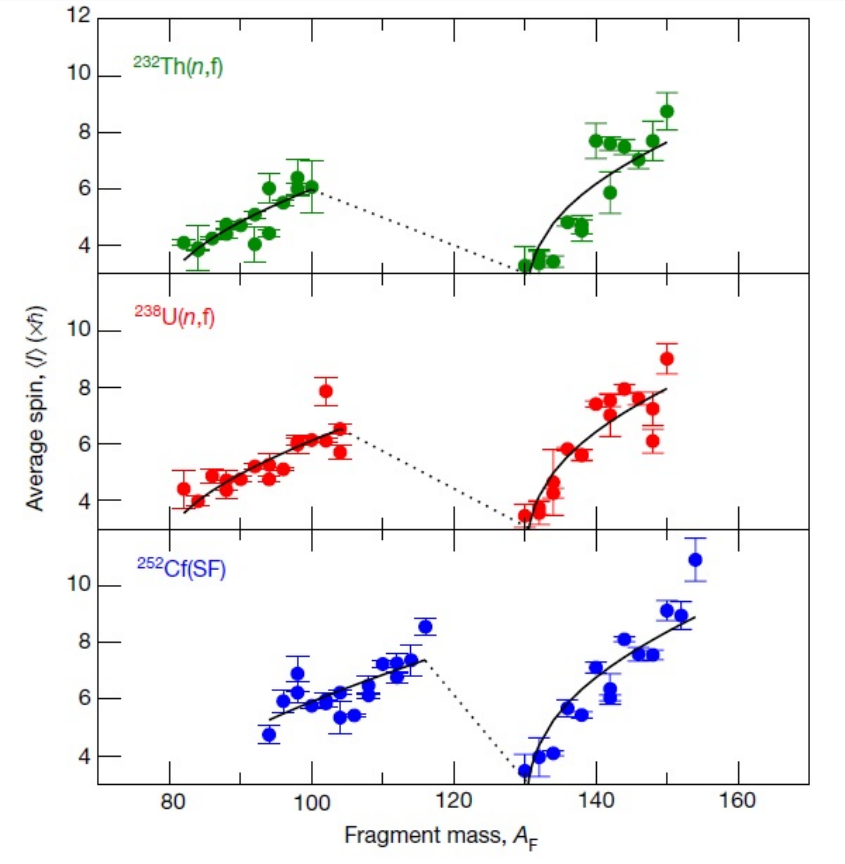

Sawtooth behavior of spin versus mass distribution

Spins vs TKE

N. P. Giha *et al.*, Phys. Rev. C, **111** 014605 (2025).

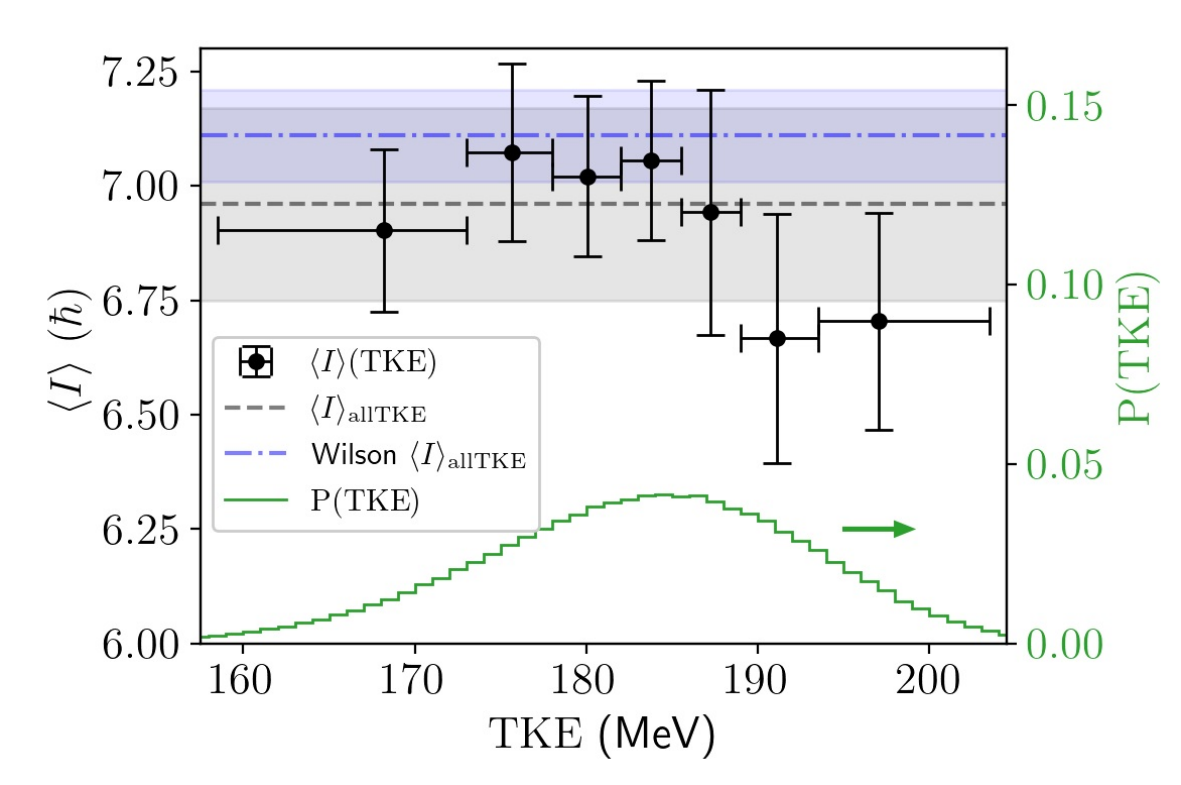

- Most energy available at scission is stored in deformation of the fragments?

Scission point model with random walk

- After crossing the fission barrier, the fissioning nucleus is treated as a superposition of various dinuclear systems.
- DNS is a system of two fragments in touching configuration characterized by their charges, masses, and deformations.
- The potential energy of DNS as a function of relative distance coordinate *R* has a pocket in the vicinity of touching configuration.
- The decay of DNS competes with an evolution in mass/charge asymmetry coordinates and in deformation of the fragments.

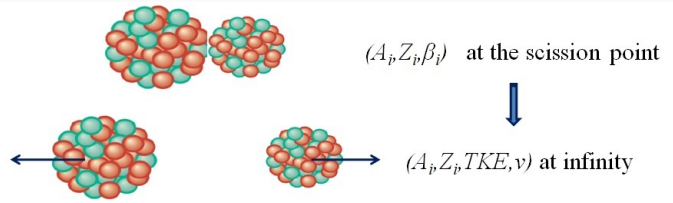

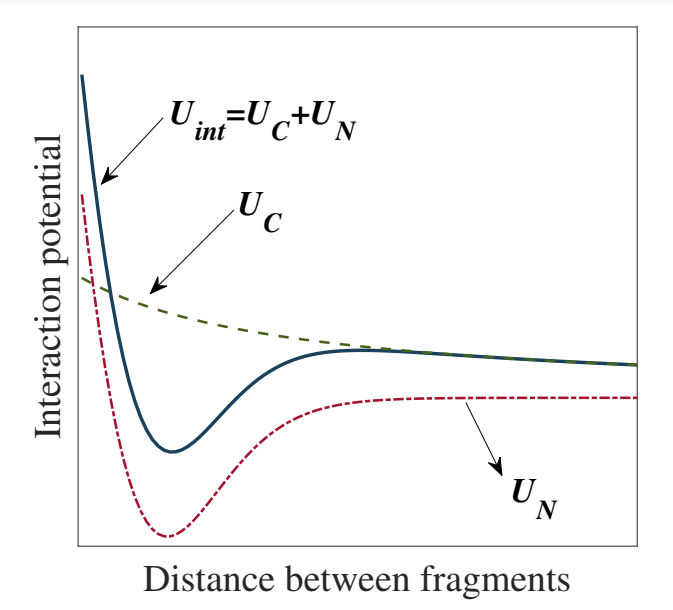

Evolution of fissioning nucleus after crossing the fission barrier

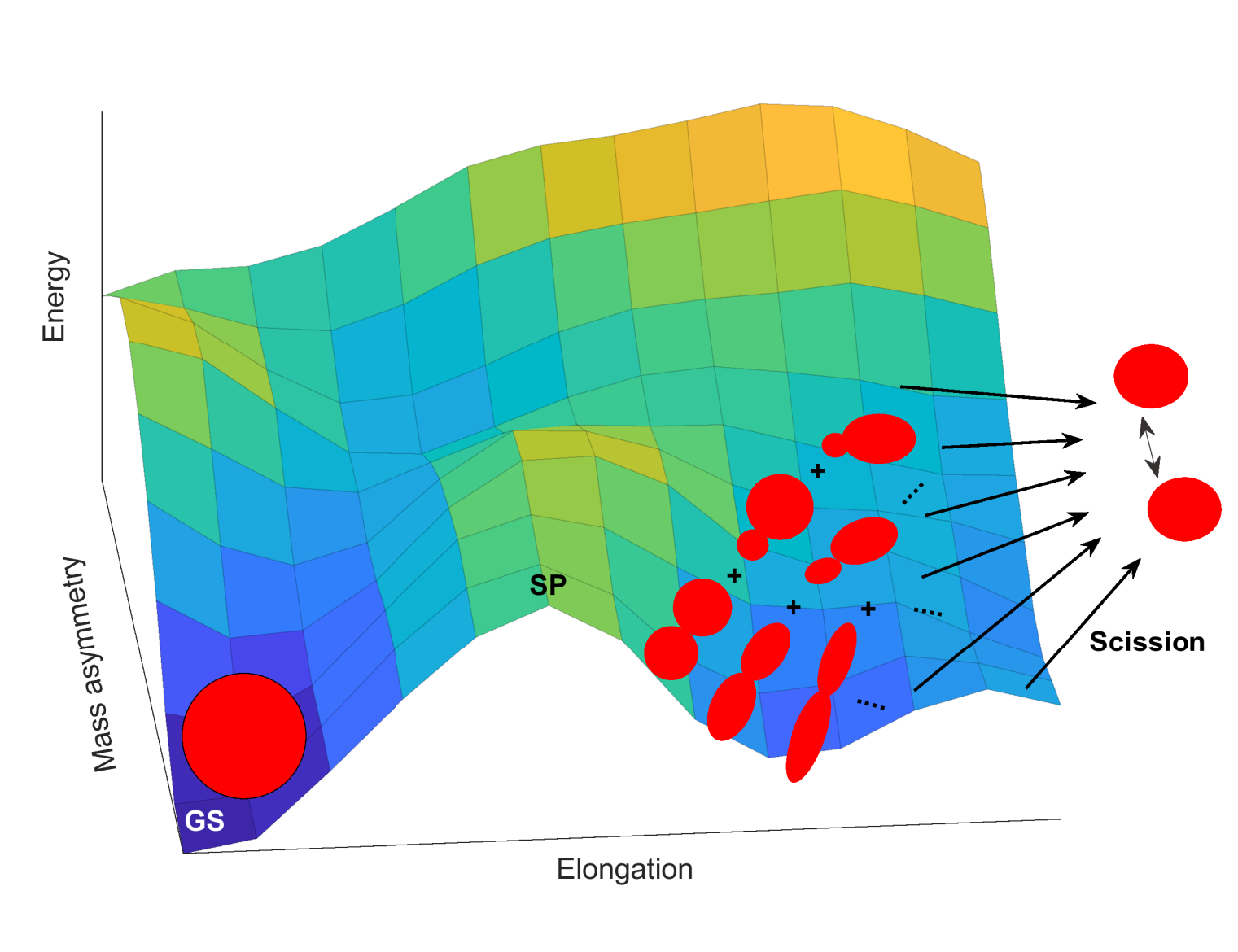

Evolution of fissioning nucleus after crossing the fission barrier

The evolution of DNS distribution in time is described using the master equation:

$$n = (Z_1, A_1, \beta_1, Z_2, A_2, \beta_2).$$

$$\frac{dP(n)}{dt} = \sum_{n' \neq n} \Lambda(n'|n)P(n') - \sum_{n' \neq n} \Lambda(n|n')P(n) - \Lambda_d(n)P(n)$$

$P(n)$ – Probability that the system is in the state n.
$P_0(n) = P(n, t = 0)$ – Probabilities of initially-formed DNS.
$\Lambda(n|n')$ – Transition rates for switching from n to n'.
$\Lambda_d(n)$ – Decay rates.

The distribution of primary fission fragments

$$P_f(n[Z_1, A_1, \beta_1, Z_2, A_2, \beta_2])$$

is obtained with Monte-Carlo technique.

Transition rates

The transition rates are expressed in terms of the microscopic transition probabilities and of the level densities of the final state.

$$\Lambda(n|n') = \lambda_{nn'}\rho(E^*_{n'}, n'), \quad \Lambda(n'|n) = \lambda_{n'n}\rho(E^*_n, n)$$

$$\lambda_{n'n} = \lambda_{nn'} = \lambda^{(i)}/\sqrt{\rho(n')\rho(n)}; \quad i = (m.a., \beta)$$

$$\Lambda_d(n) = \lambda_d \rho_{s.p.}(E^* - V_B, n)$$

$$\lambda_d = \begin{cases} 1/\sqrt{\rho_{s.p.}(n)\rho(n)}, & \text{if } (E^* > V_B) \\ 0, & \text{if } (E^* < V_B) \end{cases}$$

L.G. Moretto and J.S. Sventek, Phys. Lett. B **58**, 26 (1975).
G.G. Adamyan, A.K. Nasirov, N.V. Antonenko, R.V. Jolos , Fiz. Elem. Chastits At.Yadra **25**, 1379 (1994).

Level densities of DNS

The intrinsic level density (LD) of DNS:

$$\rho_{int}(E^*, n) = \int \rho_1(A_1, Z_1, \beta_1, \varepsilon)\rho_2(A_2, Z_2, \beta_2, E^* - \varepsilon)\mathrm{d}\varepsilon.$$

The LD of DNS fragments is calculated in superfluid formalism.

The DNS level density is obtained as a folding of intrinsic LD and the density of collective states:

$$\rho(E^*, n) = \sum_x \rho_{int}(E^* - E_x^n, n).$$

P. Decowski, et al., Nucl. Phys. A **110**, 129 (1968).

A. Bezbakh, et al., EPJA, **52**, 353 (2015).

A. Rahmatinejad, et al, Phys. Rev. C, **101**, 054315 (2020).

Choice of distribution of initial states

We choose the systems whose mass quadrupole moment lies in the interval of 10% around the value of quadrupole moment of ellipsoid with axis ratio $a : b$.

$Q_2^{ellips} \sim a : b$

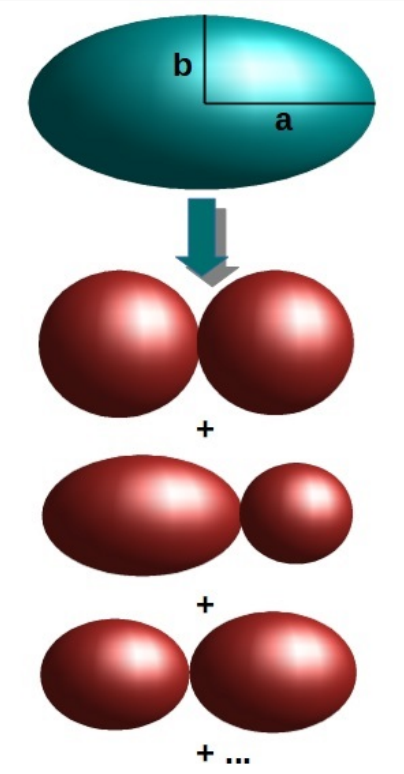

$Q_2 \sim Q_2^{ellips} \pm 10\%$

- **Probability of each DNS**

$$P_0(n) \sim \rho(n, E^* = U_{comp} - U_{DNS})$$

- **Quadrupole moment of DNS**

$$Q_2(n) = 2\frac{A_1 A_2}{A} R^2 + Q_2(A_1, \beta_1) + Q_2(A_2, \beta_2)$$

Various calculations show that nucleus can be presented as a DNS around $Q_2^{ellips} \sim 3 : 1$.

S. Cwiok, W. Nazarewicz et al., PLB, **322**, 304 (1994).
T. M. Shneidman et al., NPA, **671**, 119 (2000).
A. V. Afanasjev et al., Phys. Scr. **93**, 034002 (2018).

Neutron multiplicity

After decay of DNS, fragments shrinks to their ground state releasing its deformation energy:

$$E_i^{def}(n) = \left[U_i^{LD}(Z_i, A_i, \beta_i) + E_i^{sh}(Z_i, A_i, \beta_i)\right] - \left[U_i^{LD}(Z_i, A_i, \beta_i^{gs}) + E_i^{sh}(Z_i, A_i, \beta_i^{gs})\right]$$

Excitation energies of fragments at scission:

$$\left(\frac{1}{\rho_1(\varepsilon)}\frac{d\rho_1(\varepsilon)}{d\varepsilon}\right)\Bigg|_{\varepsilon=E_1^*} = \left(\frac{1}{\rho_2(\varepsilon)}\frac{d\rho_2(\varepsilon)}{d\varepsilon}\right)\Bigg|_{\varepsilon=E_2^*} = T^{-1}.$$

Neutron multiplicity:

$$Y(\nu) = \sum_j \left[\sum_{x=1}^{\nu} F_1(x, E_1^{def}(n_j) + E_1^*(n_j)) F_2(\nu - x, E_2^{def}(n_j) + E_2^*(n_j))\right] P_f(n_j).$$

$F_{1,2}(x, E_{1,2})$ – probabilities to emit exactly x neutrons.

Neutron multiplicities of $Z \sim 100$ nuclei

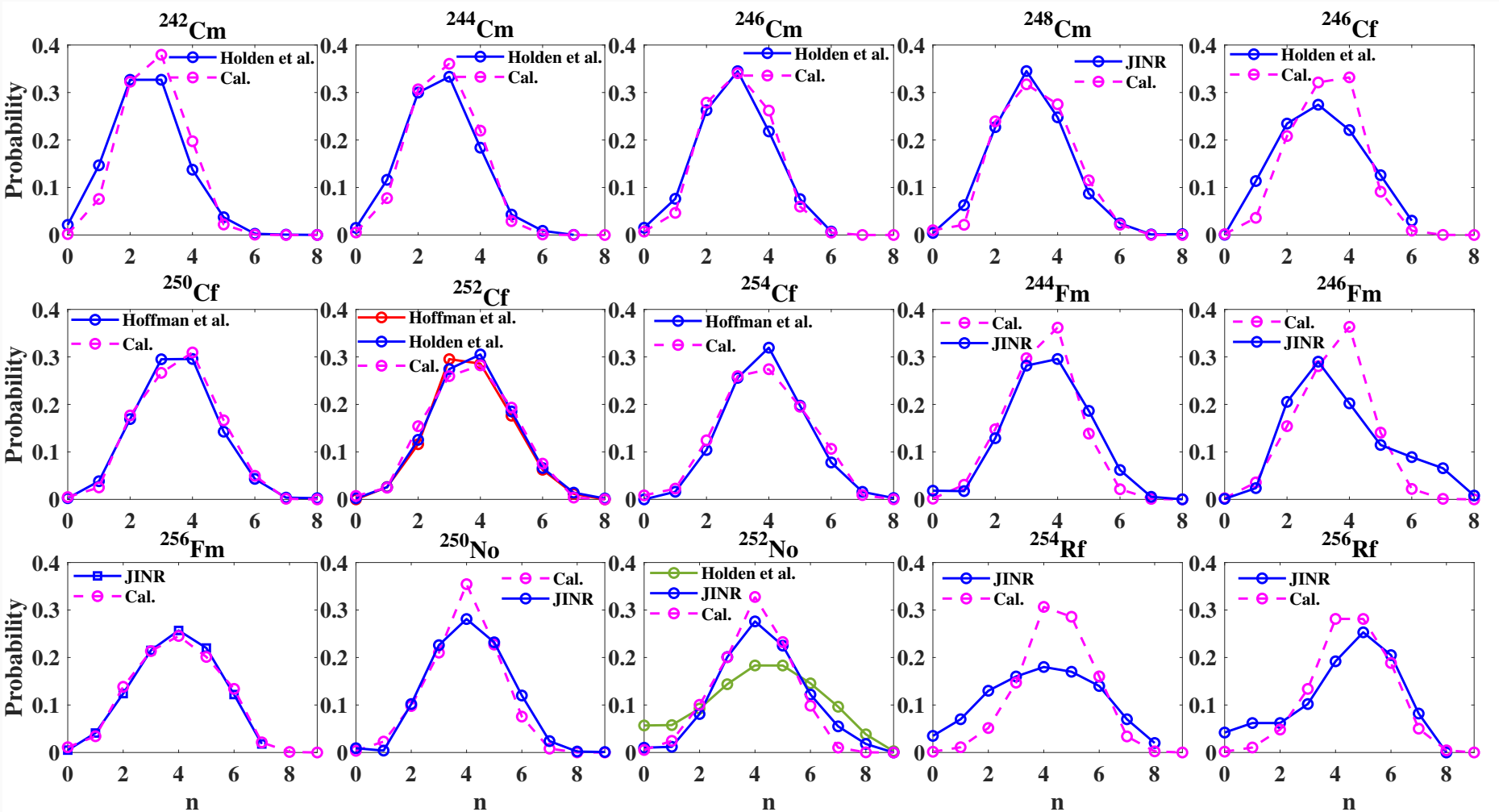

$\lambda^{(A)} = 1.7; \lambda^{(\beta)} = 1.2; Q_{init} \sim 3.2 : 1$

^{256}Rf: Mass distribution

solid line – overall;
squares: 0n – 1n;
circles: 2n – 3n;
triangles: 4n – 5n
rhombus: 6n – 9n.

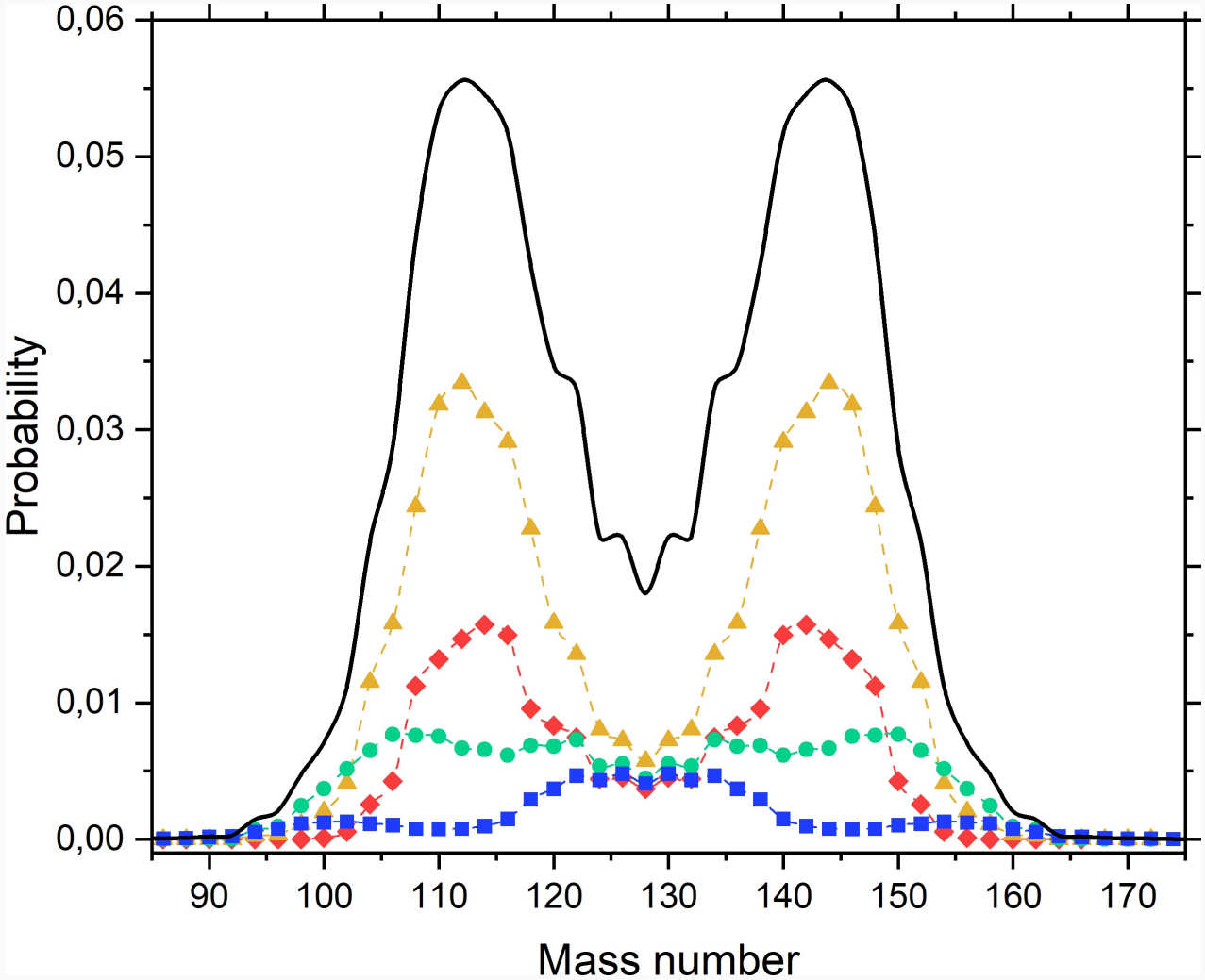

A.V. Isaev, et al., PLB **843**, 138008 (2023).

Mass distribution in SF of even $^{244-260}$Fm isotopes

$$Y(A) = \sum_{n_j} P_f(n_j)\left[\delta_{A_1,A} + \delta_{A_2,A}\right], \quad Y(Z) = \sum_{n_j} P_f(n_j)\left[\delta_{Z_1,Z} + \delta_{Z_2,Z}\right].$$

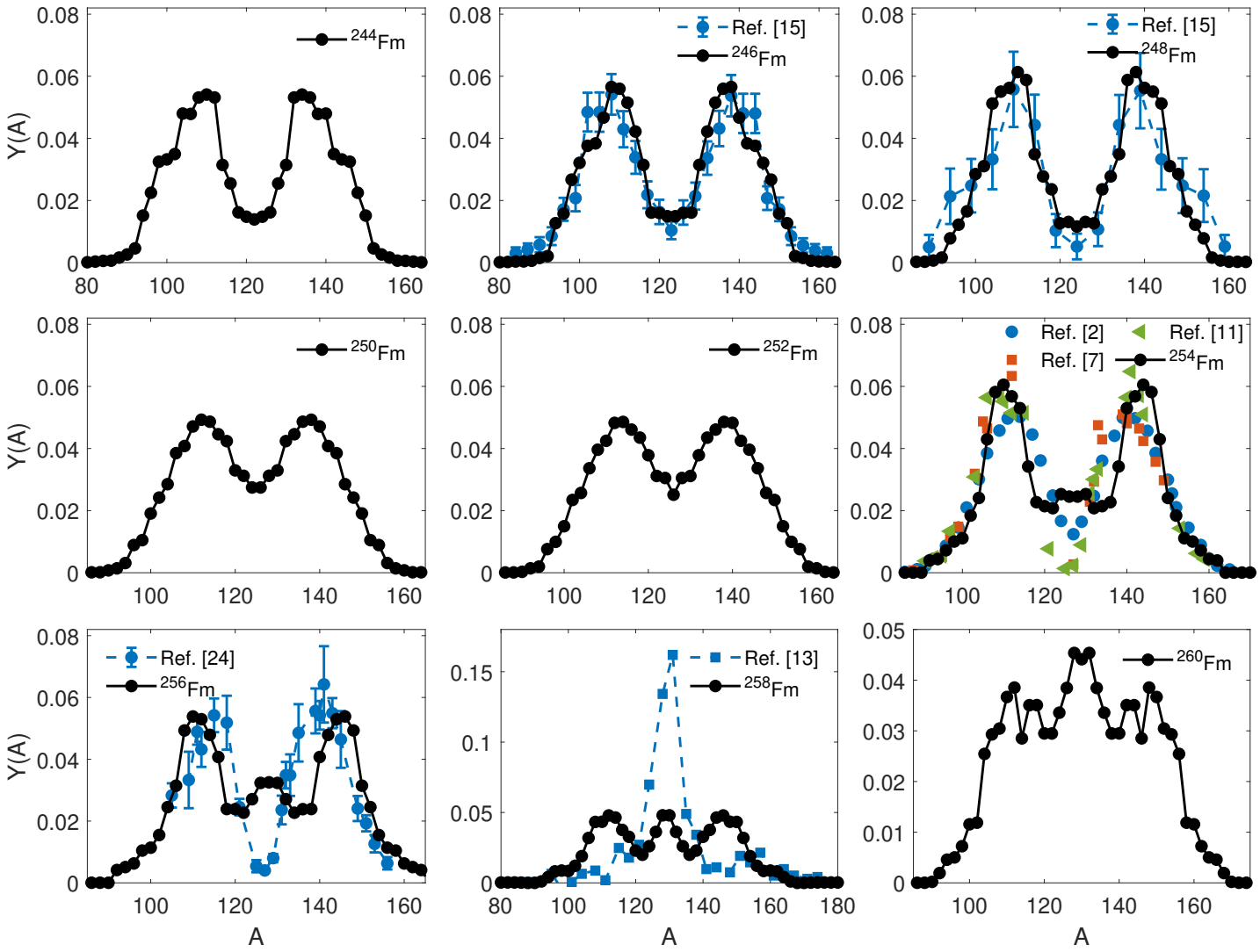

Mass/Charge distribution in ^{258}Fm

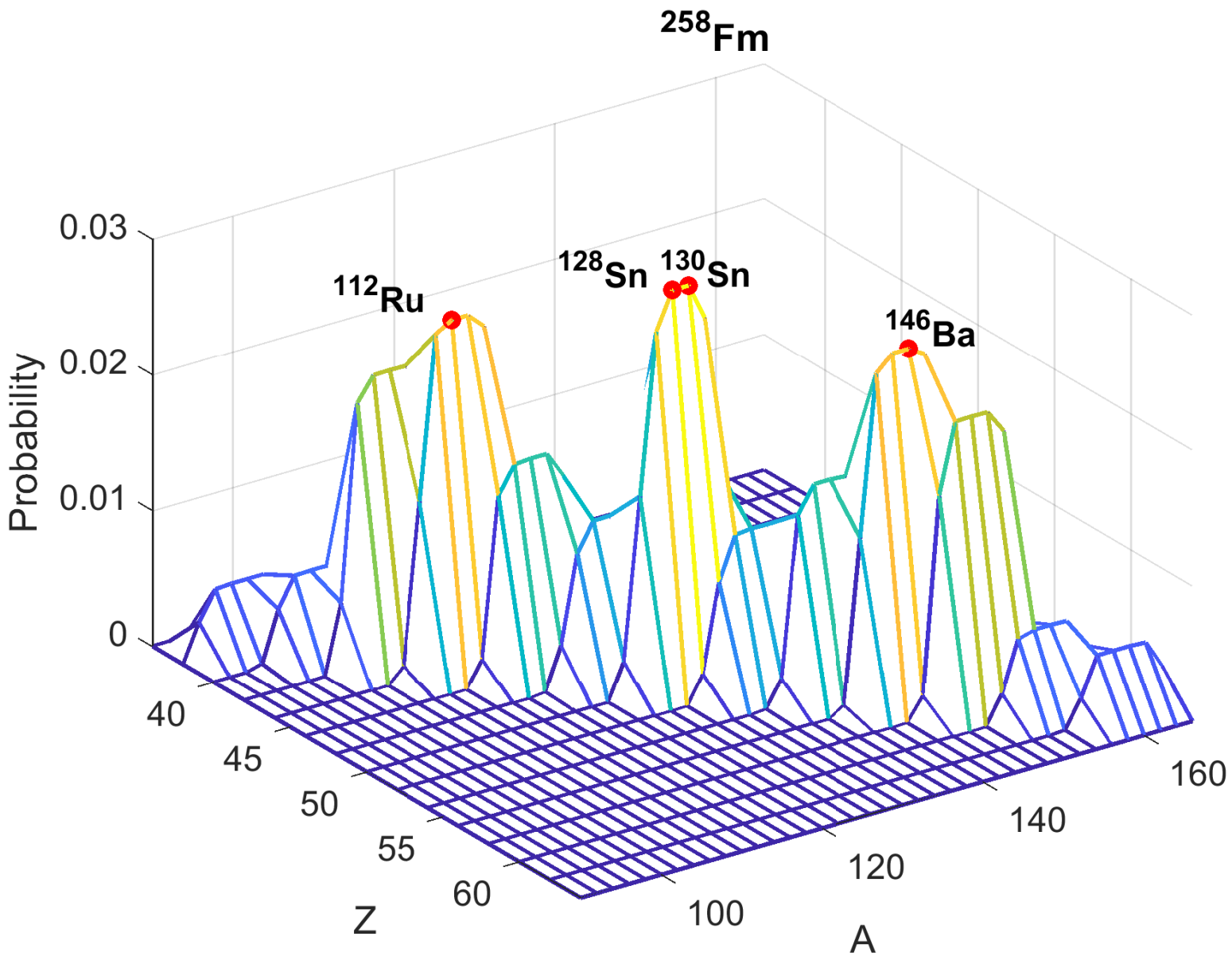

Scission configurations in SF of ^{258}Fm

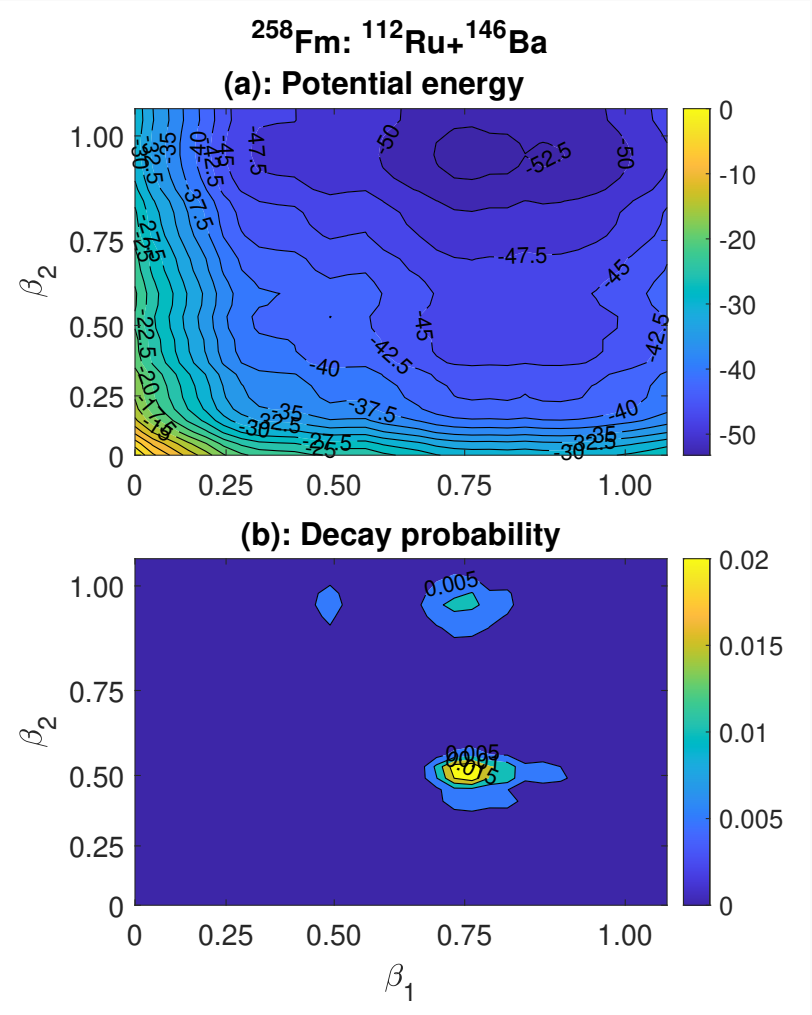

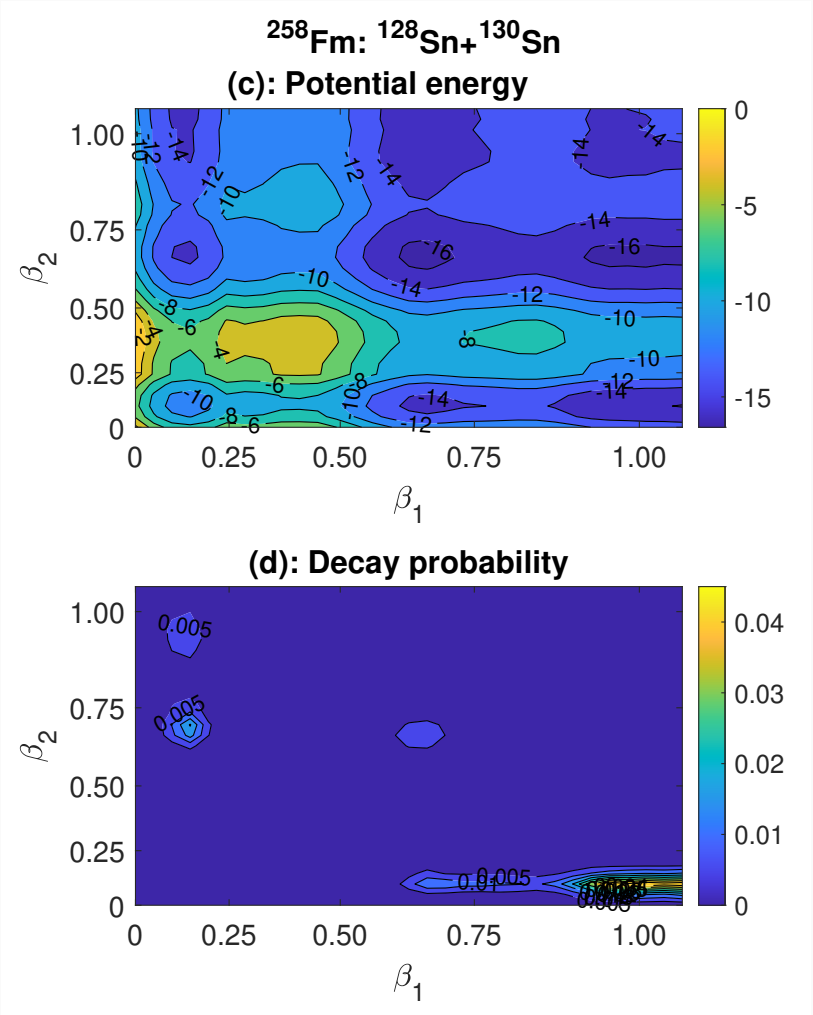

Half-lives of Fermium isotopes

Isotope	β_2 of SP	Fission barrier height (MeV)	Exp. SF half-lives
^{244}Fm	0.44	6.07	3.2165 ms
^{246}Fm	0.44	6.61	22.6471 s
^{248}Fm	0.44	6.89	9.5833 h
^{250}Fm	0.45	6.99	301.9292 day
^{252}Fm	0.45	6.98	126.0166 year
^{254}Fm	0.45	6.21	228.0417 day
^{256}Fm	0.45	5.40	2.8491 h
^{258}Fm	0.41	4.82	370 μs
^{260}Fm	0.57	4.55	-
^{262}Fm	0.57	4.74	-

Fission barriers: P. Jachimowicz, M. Kowal, and J. Skalski, At. Data Nucl. Data Tables **138**, 101393, (2021).

Half lives: www.nndc.bnl.gov/ensdf

Compact SF of ^{258}Fm

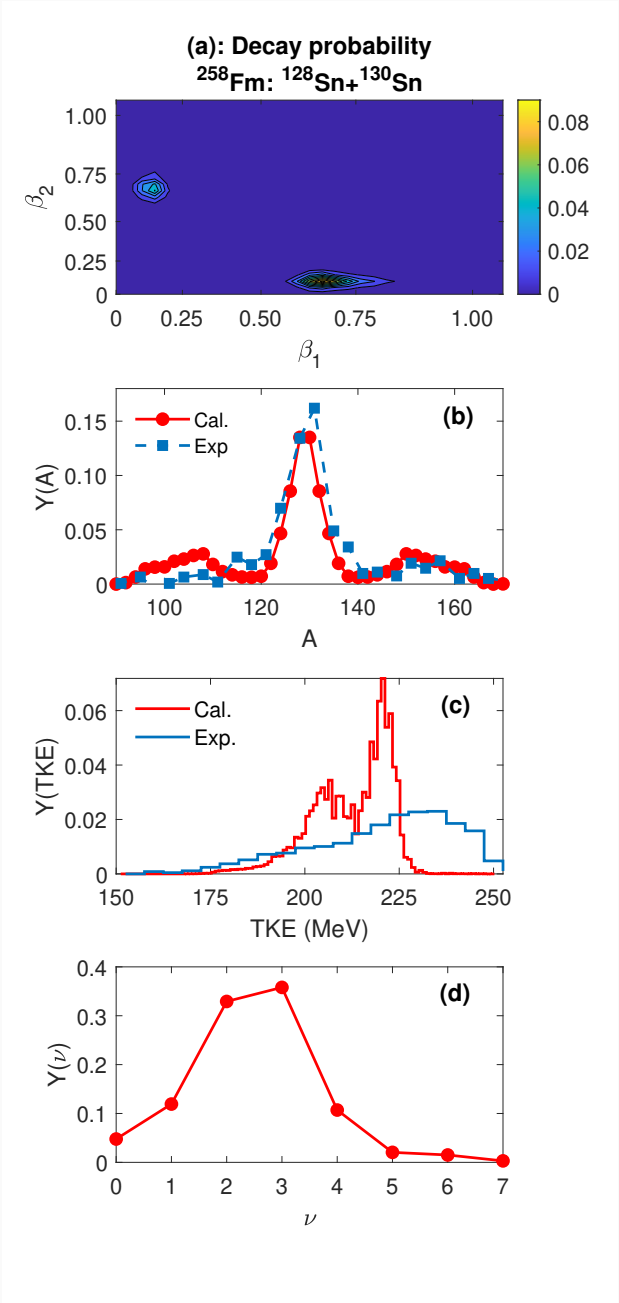

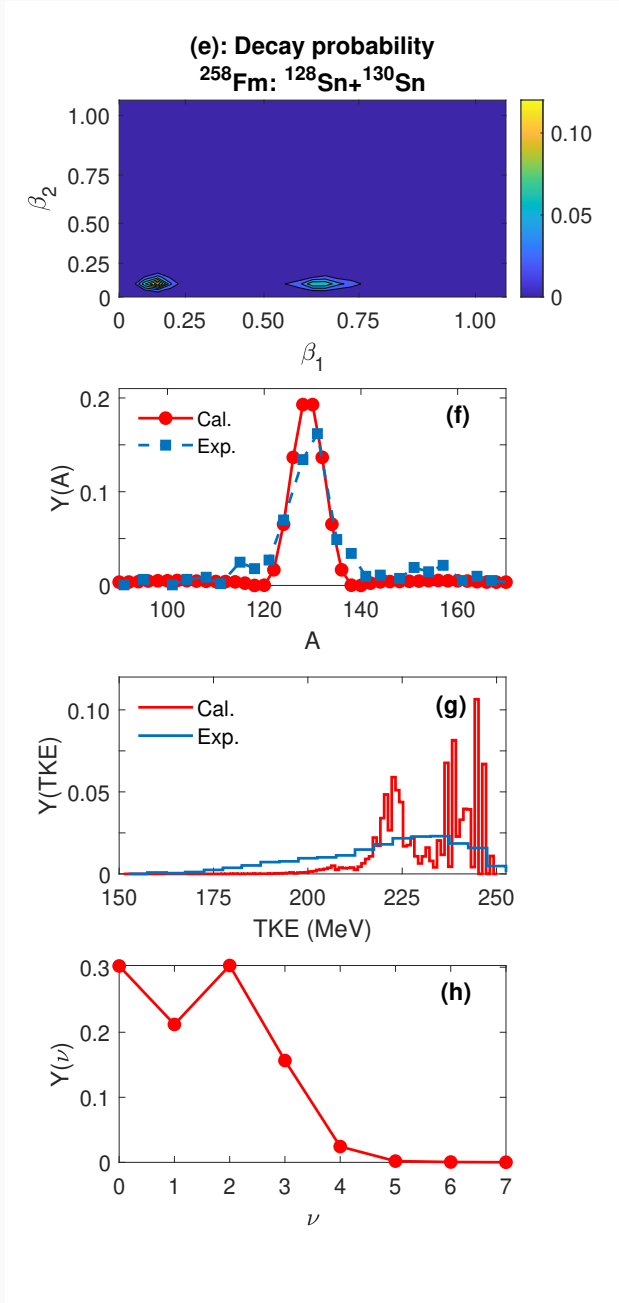

Exp. data:
D. C. Hoffman et. al, PRC, **21**, 972 (1980).
E. K. Hulet et. al, PRC **40**, 770 (1989).

Angular motion at scission

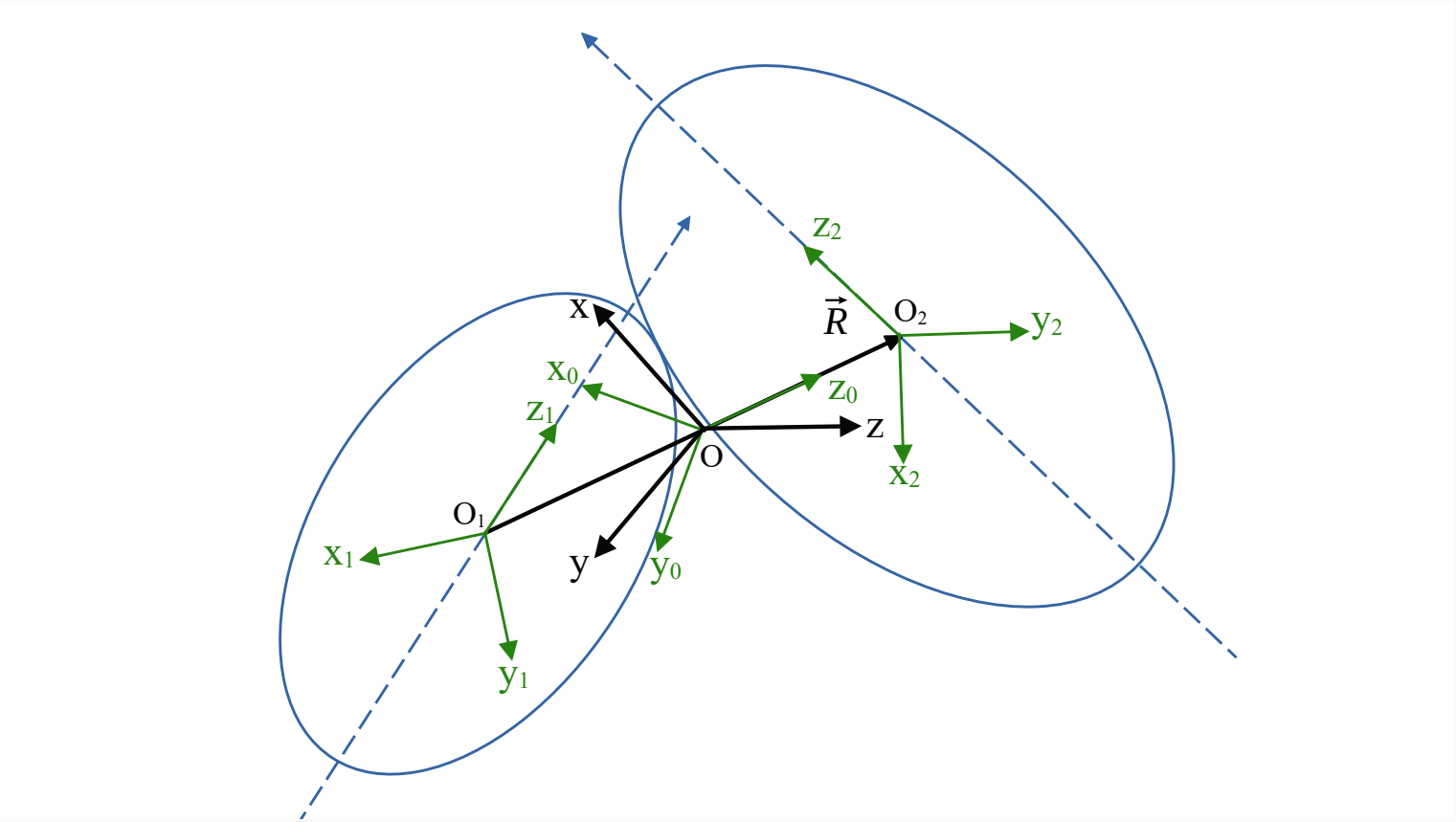

$\Omega_{1,2} = (\phi_{1,2}, \theta_{1,2}, 0)$ – orientation of fragments with respect to the lab. system

R$= (R, \theta_R, \phi_R)$ – vector connecting centers of the fragments.

Hamiltonian of angular motion in DNS

Kinetic energy:

$$T = \frac{\hbar^2 \hat{I}_0^2}{2\mu R_m^2} + \frac{\hbar^2 \hat{I}_1^2}{2\Im_1} + \frac{\hbar^2 \hat{I}_2^2}{2\Im_2}$$

Angular momentum operators:

$$\hat{I}_i^2 = -\left(\frac{1}{sin\theta_i}\frac{\partial}{\partial\theta_i}sin\theta_i\frac{\partial}{\partial\theta_i} + \frac{1}{sin^2\theta_i}\frac{\partial^2}{\partial\phi_i^2}\right), \quad \hat{I}_i^2 Y_{I_iM_i}(\Omega_i) = I_i(I_i+1)Y_{I_iM_i}(\Omega_i)$$

$\Im_{1,2}$: moments of inertia of fragments.
$\Im_R = \mu R_m^2$: moment of inertia of relative motion.

Potential energy:

$$V(R, \tilde{\Omega}_1, \tilde{\Omega}_2) = V_N(R_m, \tilde{\Omega}_1, \tilde{\Omega}_2) + V_{coul}(R_m, \tilde{\Omega}_1, \tilde{\Omega}_2), \quad \tilde{\Omega}_i = (\varepsilon_i, \gamma_i, 0)$$

$$V(\Omega_1, \Omega_2, \Omega_0) = \sum_{\lambda_0,\lambda_1,\lambda_2} V_{\lambda_0,\lambda_1,\lambda_2}\left[Y_{\lambda_0}(\Omega_0) \times [Y_{\lambda_1}(\Omega_1) \times Y_{\lambda_2}(\Omega_2)]_{\lambda_0}\right]_{(00)}$$

Potential energy

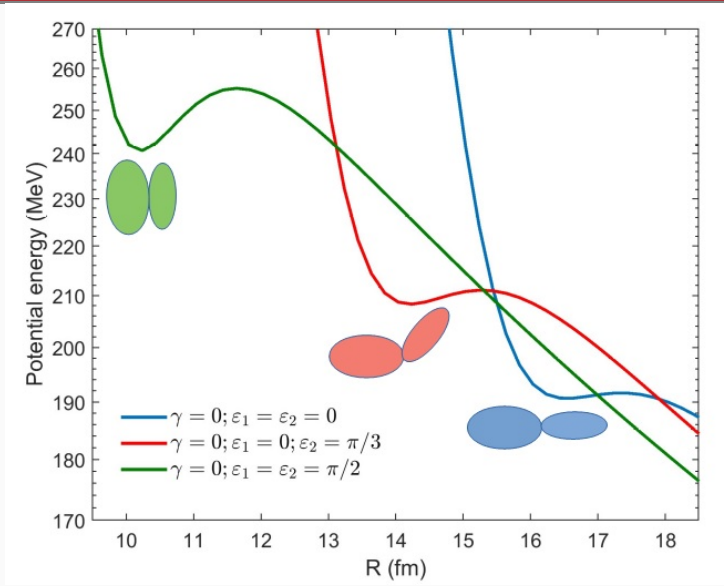

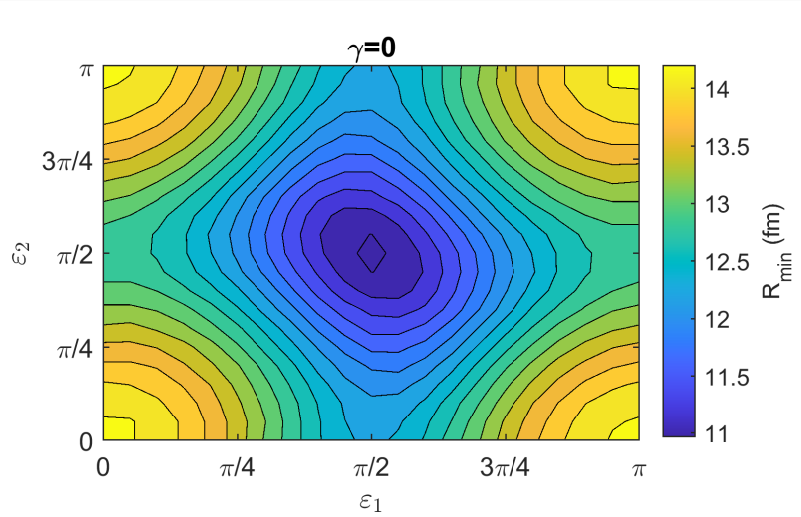

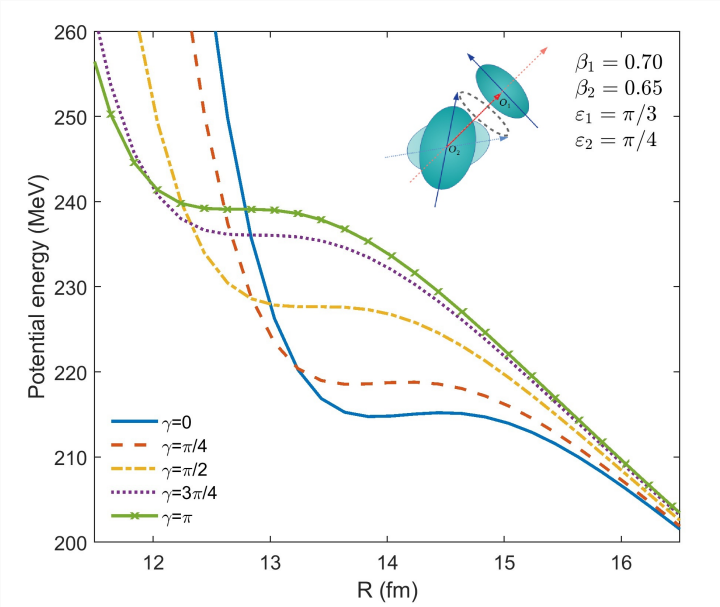

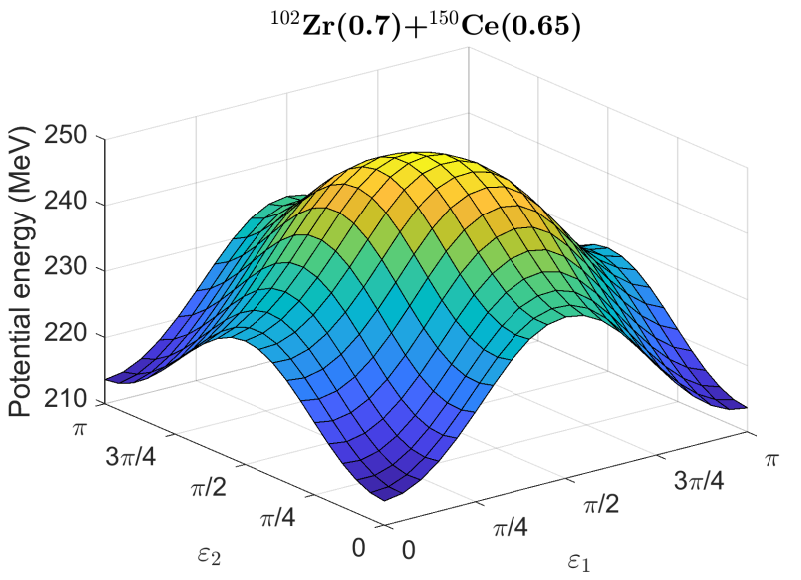

Basis

For a given total angular momentum I and its projection M, Hamiltonian is diagonalized on the set of tripolar spherical functions.

$$[i_0 \times [i_1 \times i_2]_{i_{12}}]_{(I,M)} \equiv \left[Y_{i_0}(\Omega_0) \times [Y_{i_1}(\Omega_1) \times Y_{i_2}(\Omega_2)]_{i_{12}}\right]_{(I,M)}$$

$$= \sum_{m_0 m_1 m_2 m_{12}} C^{IM}_{i_0 m_0, i_{12} m_{12}} C^{i_{12} m_{12}}_{i_1 m_1, i_2 m_2} Y_{i_0 m_0}(\Omega_R) Y_{i_1 m_1}(\Omega_1) Y_{i_2 m_2}(\Omega_2)$$

$$\psi^n_{IM} = \sum_{i_0 i_1 i_2 i_{12}} a^n_{i_0 i_1 i_2 i_{12}} \left[i_0 \times [i_1 \times i_2]_{i_{12}}\right]_{(IM)}$$

$\mathcal{P}(i_0 i_1 i_2) = \sum_{i_{12}} |a_{i_0 i_1 i_2 i_{12}}|^2$: Probability that angular momentum of first fragment is i_1, of second fragment is i_2, and relative angular momentum is i_0.

$$\langle I_i \rangle_n = \left[\sum_{I_0 I_1 I_2} I_i(I_i+1)\mathcal{P}(I_0 I_1 I_2)\right]^{1/2} \qquad i = 0, 1, 2$$

Excitation spectrum of angular vibrations

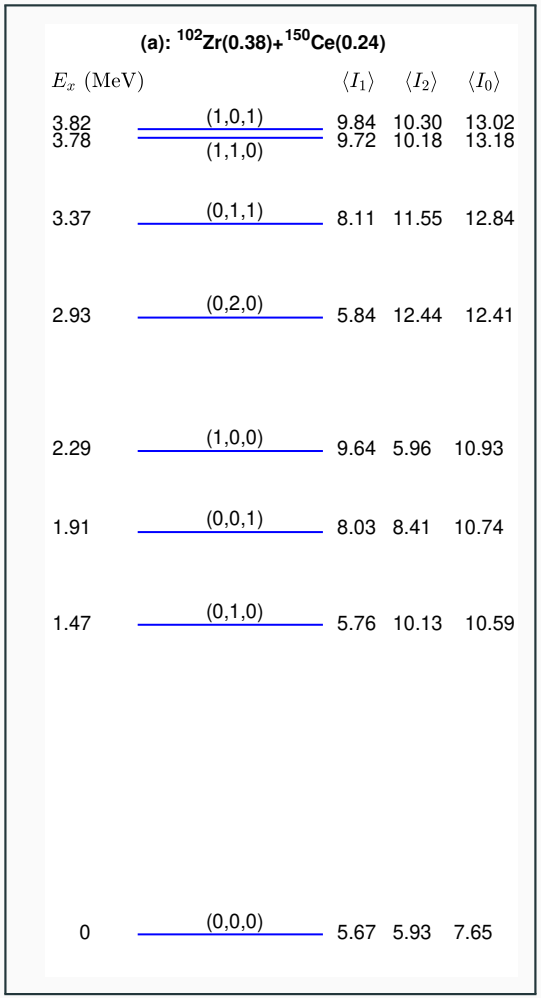

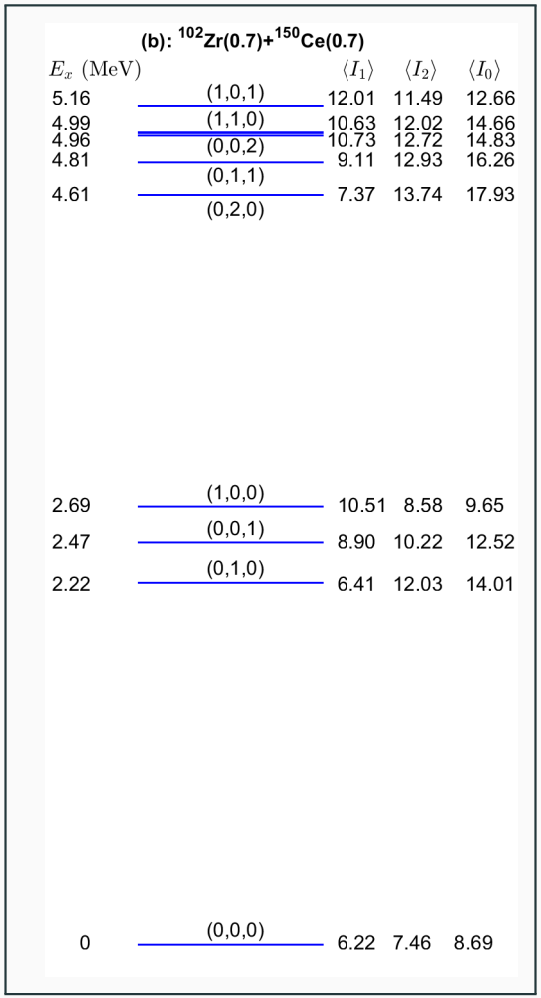

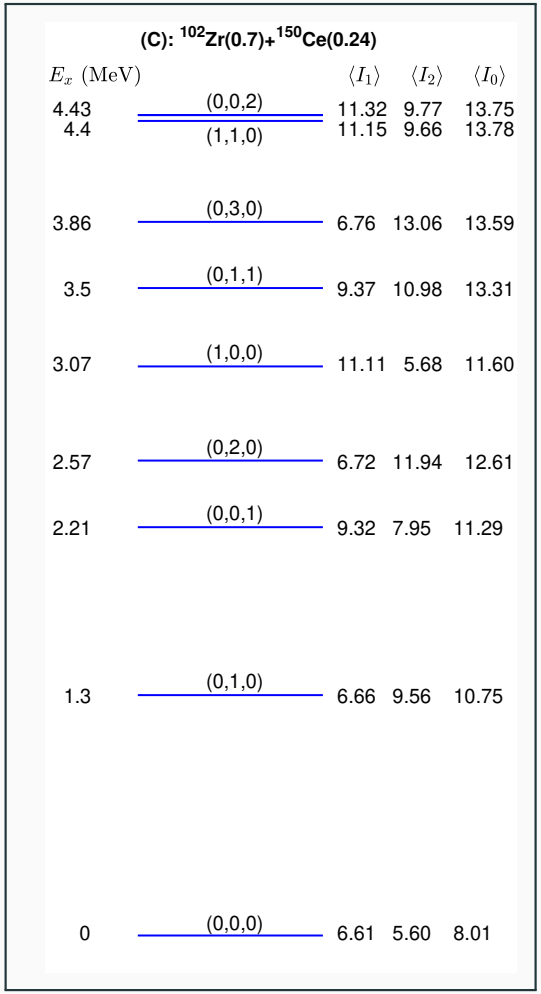

$$E_{n_1,n_2,\bar{K}} = \hbar\omega_1(2n_1 + |\bar{K}| + 1) + \hbar\omega_2(2n_2 + |\bar{K}| + 1), \quad \omega_i = \sqrt{C_i/\Im_{b,i}}$$

$$\Im_{b,i} = (1/\Im_0 + 1/\Im_i)^{-1} \approx \Im_i$$

T. M. Shneidman et al., Phys. Rev. C **92**, 034302 (2015).

Correlation between fragments angular momenta

$$\langle I_1 \rangle_n = \left[\sum_{i_0, i_1, i_2 \geq I_{min}} |a^{(n)}_{i_0 i_1 i_2}|^2 i_1(i_1+1) \right]^{1/2}$$

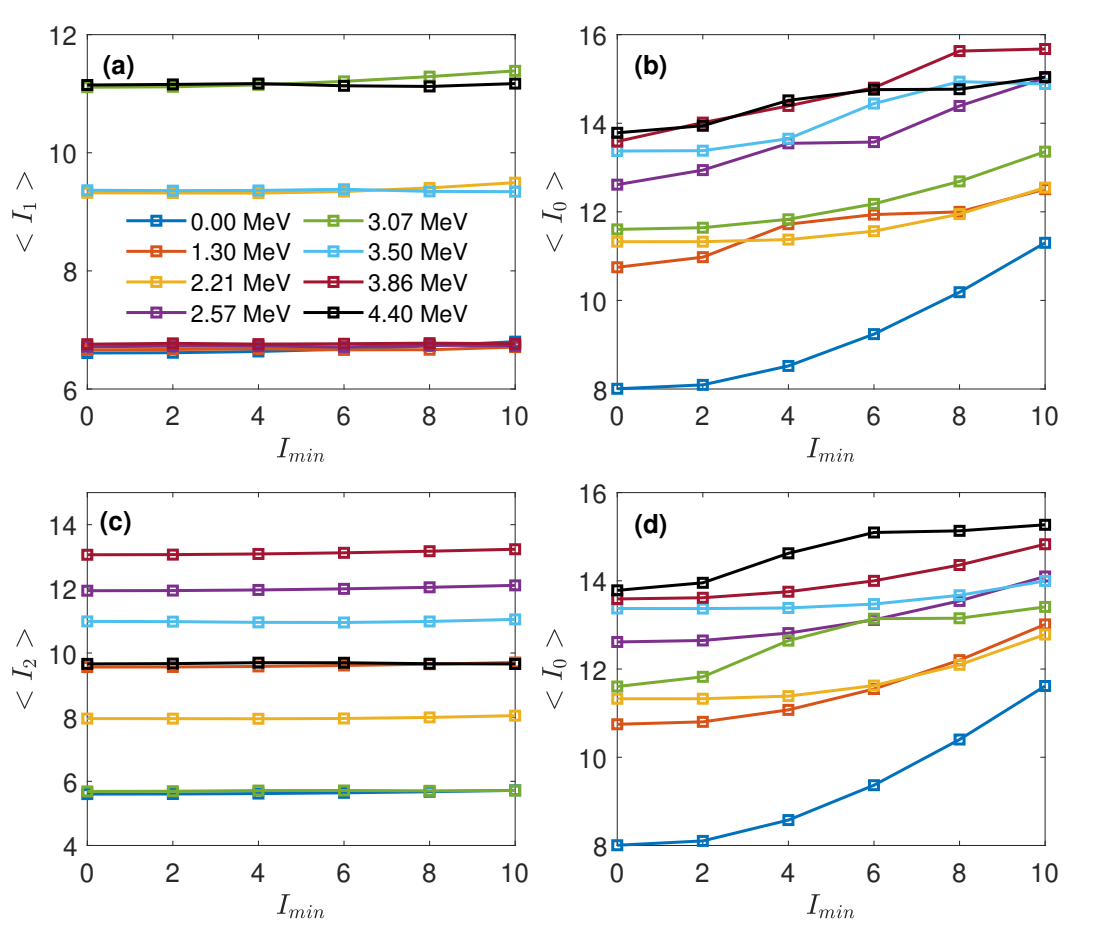

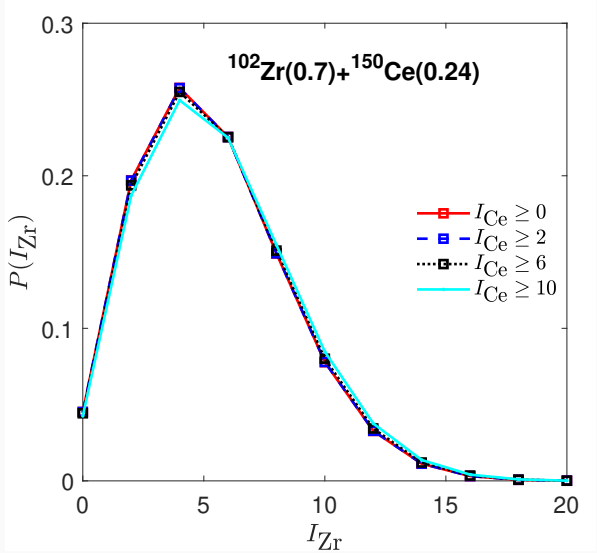

In previous studies rotation of fissile nucleus as a whole was not taken into account.

$I_0 + I_1 + I_2 = 0, \quad \Im_0 \gg \Im_{1,2}$

T. M. Shneidman et al., PRC **111**, (2025).

The role of deformation $\longrightarrow$ Saw-tooth behavior

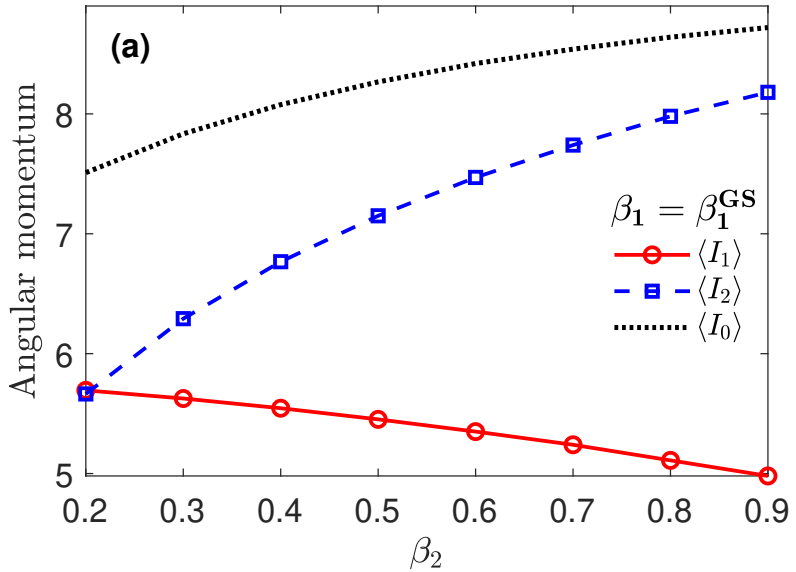

Average distortion angle:

$$\overline{\varepsilon_i} = \sqrt{\langle \varepsilon_i^2 \rangle} \sim \hbar (C_i \Im_i)^{-1/4}$$

Uncertainty relation $\longrightarrow \langle I \rangle \sim (C_i \Im_i)^{1/4}$

$$C_i \sim Z_1 Z_2 \beta_i / R_m^3(0)$$

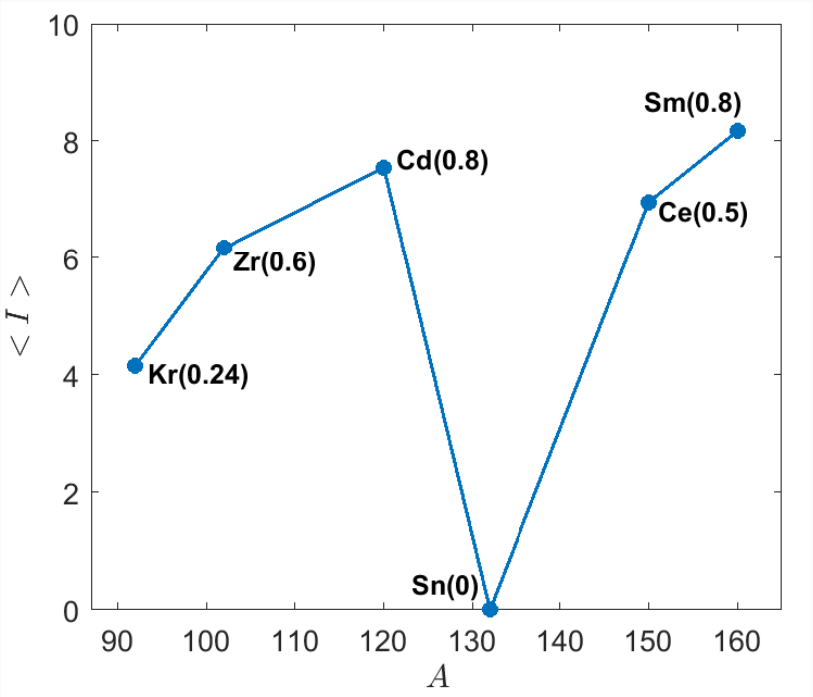

T. M. Shneidman et al., PRC **111**, (2025).

Scission configurations leading to ^{144}Ba fission fragment

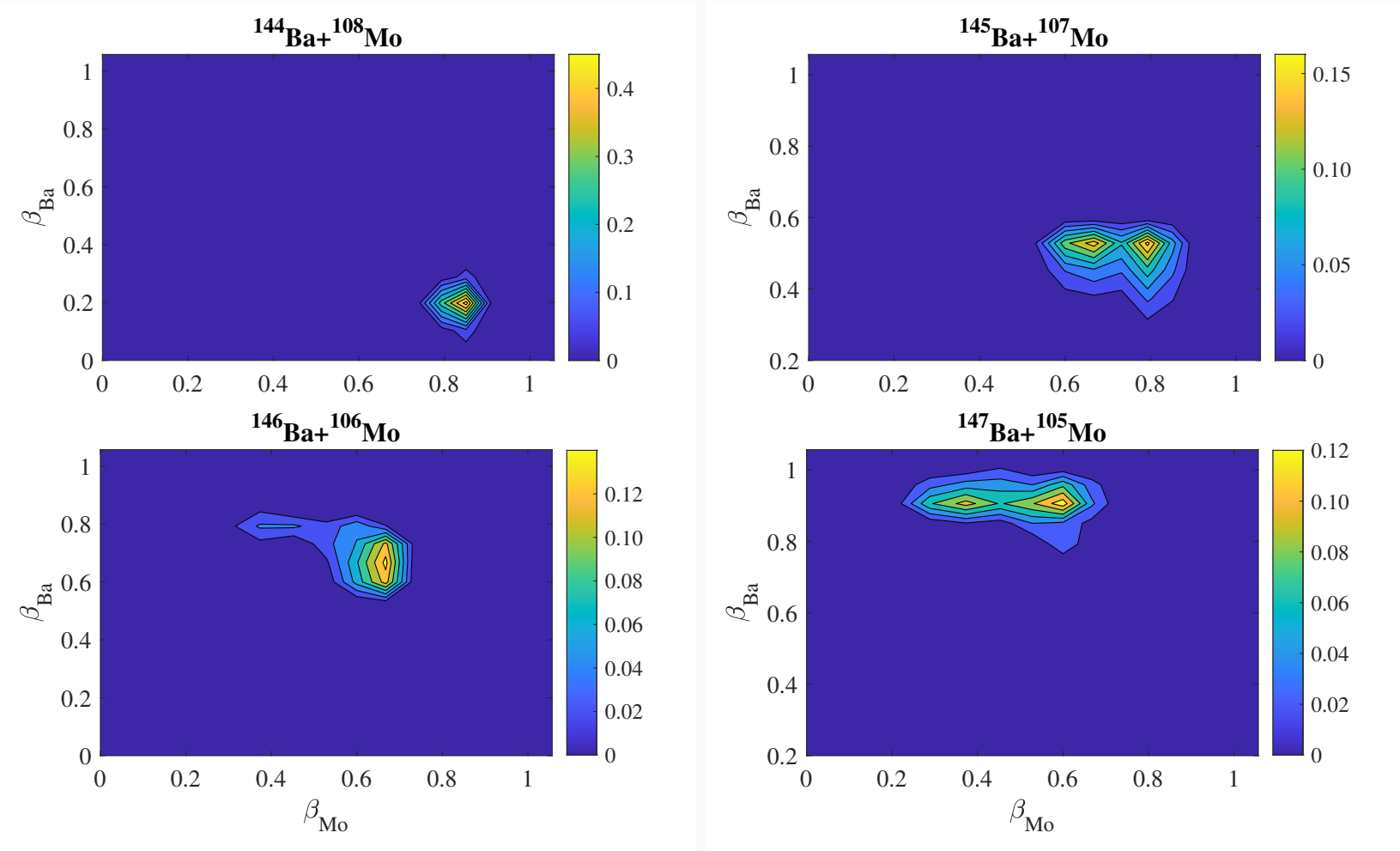

The decay probabilities of scission configurations leading to post-scission fragment ^{144}Ba as a function of the deformations β_{Mo} and β_{Ba} of the Mo and Ba fragments.

TKE distribution for various scission configurations

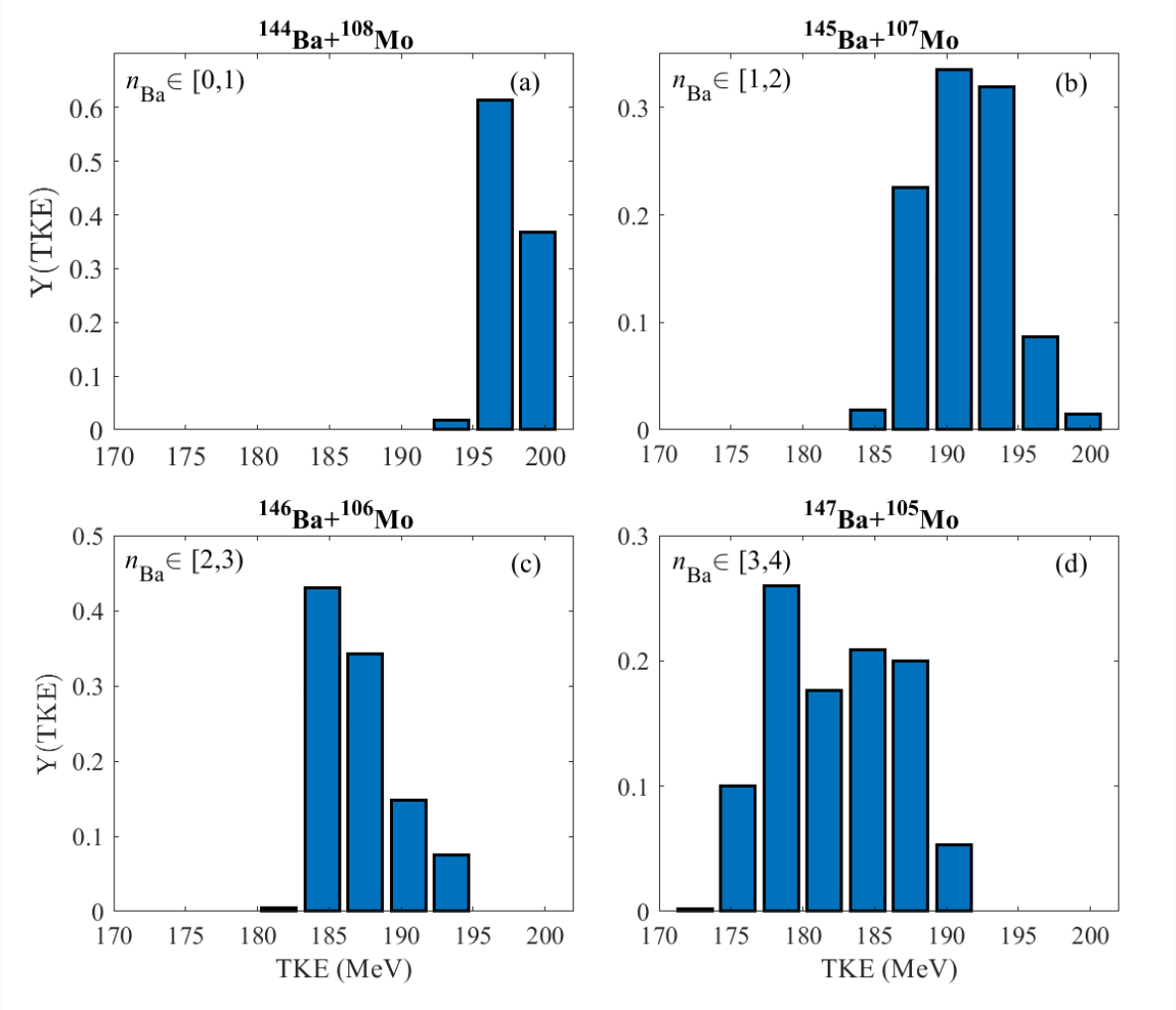

The calculated total kinetic energy distributions for the decay from various scission configurations leading to post-scission fragment ^{144}Ba. Each TKE distribution presented here is normalized to unity.

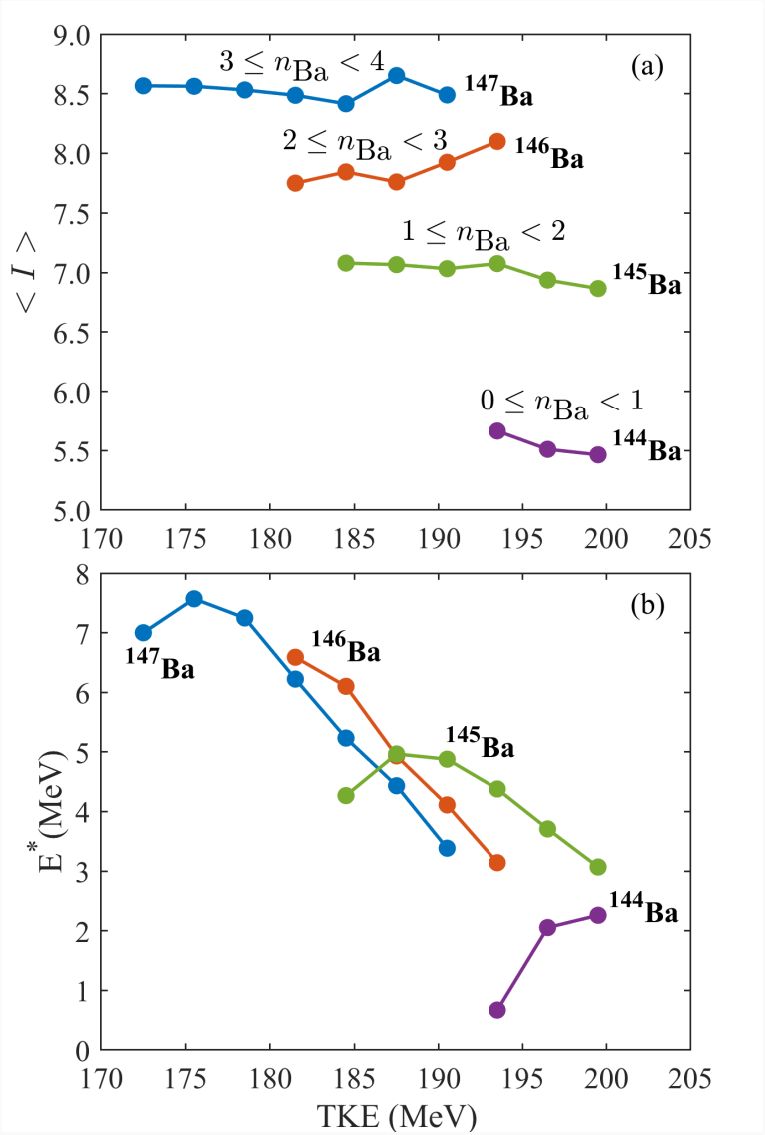

The calculated average spins and excitation energies of Ba isotopes in scission configurations leading to ^{144}Ba after n_{Ba} neutron emissions, plotted against total kinetic energy TKE.

Spin vs TKE for ^{144}Ba fragment of SF ^{252}Cf

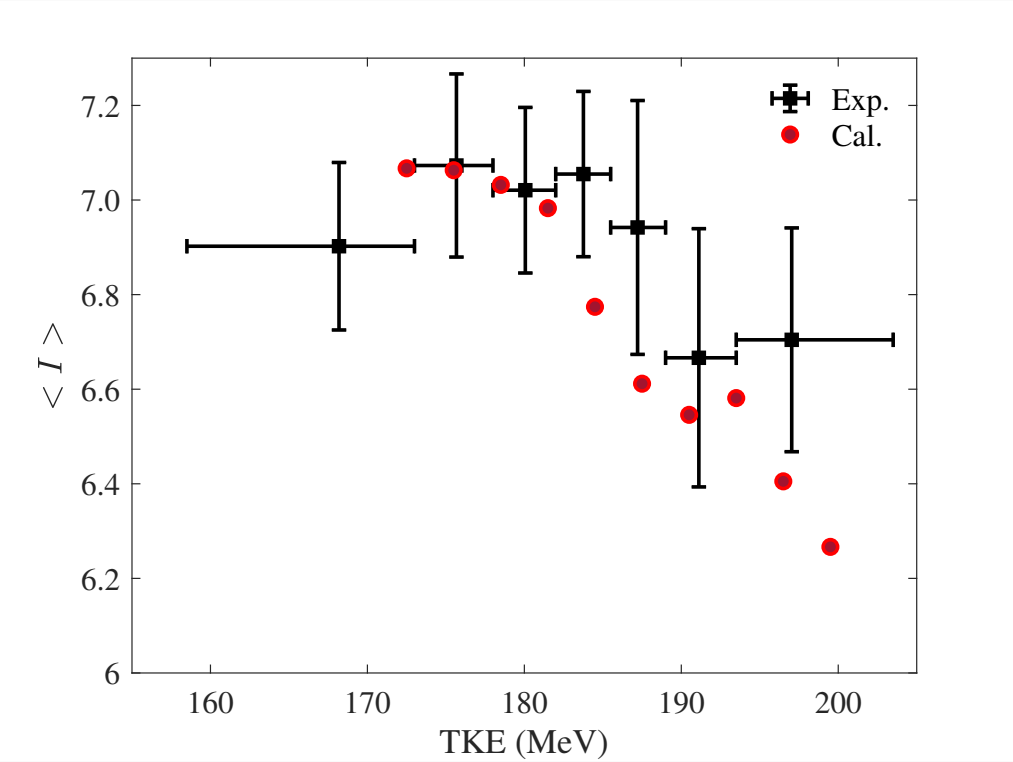

Average spins $\langle I \rangle$ of post-scission ^{144}Ba (red circles) as a function of total kinetic energy (TKE). Exp. data (black squares) from N. P. Giha *et al.*, PRC **111** 014605 (2025).

A. Rahmatinejad et al., subm. to PRC

Conclusion

- The model to describe the evolution of a fissioning nucleus after tunneling through the fission barrier as a random walk among various scission configurations is proposed.
- The prompt neutrons yield data from spontaneous fission of Z = 100–106 is described.
- Calculations of fission observables for ^{258}Fm nuclei indicate presence of bimodality due to competition between spherical (compact) and deformed mass symmetric fission modes.
- Angular motion in scission configuration of fissioning nucleus is described quantum-mechanically.
- The absence of correlation between the spins of FF, the sawtooth pattern in spin vs mass distribution, and recently observed weak dependence of spins of FF on TKE is explained.